Received June 1995
Revised November 1996

Natural convection in interacting cavities heated from below

A. Raji, M. Hasnaoui and Z. Zrikem
Physics Department, University of Cadi Ayyad, Marrakesh, Morocco

Nomenclature

A	=	aspect ratio of the system, L'/H'
B	=	relative height of the cavities, h'/H'
g	=	acceleration due to gravity, m^2/s
h'	=	dimensional height of the cavities, m
$\bar{h}$	=	average heat transfer coefficient on cold wall, W/m^2K
H'	=	dimensional height of the system, m
l'_1	=	length of a cavity, m
l'_2	=	length of a baffle, m
L'	=	total length of the domain, m
Nu	=	normalized mean Nusselt number
Pr	=	Prandtl number, ν/α
Q	=	overall heat transfer by convection across the cold wall
Qc	=	overall heat transfer by conduction across the cold wall
Ra	=	Rayleigh number, $g\beta\Delta T'H'^3/(\nu\alpha)$
t	=	dimensionless time, $t'\alpha/H'^2$
T	=	dimensionless temperature of fluid, $(T' - T'_C)\Delta T'$
$\Delta T'$	=	temperature difference, $T'_H - T'_C$, K
u,v	=	dimensionless velocities in x and y directions, $(u', v')H'/\alpha$
x,y	=	dimensionless Cartesian co-ordinates, $(x',y')/H'$

Symbols

λ	=	thermal conductivity, W/Km
α	=	thermal diffusivity of the fluid, m^2/s
β	=	volumetric coefficient of thermal expansion, $1/K$
Φ	=	inclination of the system
ν	=	kinematic viscosity, m^2/s
ψ	=	dimensionless stream function, ψ'/α
Ω	=	dimensionless vorticity, $\Omega' H'^2/\alpha$

Subscripts

H	=	heated wall
C	=	cooled wall
max	=	maximum value
min	=	minimum value
ext	=	extremum value

Superscript

$'$	=	dimensional variables

Note: The symbols defined above are subject to alteration on occasion

Introduction

During the last two decades, considerable efforts have been devoted to the study of natural convection flows generated by buoyancy forces in finite geometries. The interest in such problems stems from their importance in such areas as convective heat loss from solar collectors, energy conservation in buildings, air conditioning, and recently, the cooling of electronic components by natural convection. Reviews of a large part of these works have been presented by Bejan[1], Platten and Legros[2] and Yang[3]. Numerous engineering applications have made the topic of natural convection in enclosures one of the most active subfields in heat transfer research today. The existing literature in this domain has focused considerable attention on natural convection in rectangular cavities differentially heated. Some of these works have been recently

International Journal of Numerical Methods for Heat & Fluid Flow
Vol. 7 No. 6, 1997, pp. 580-597.

summarized in reviews and reference books by Catton[4]. A few investigations concerning heat and fluid flow phenomena in systems fully[5,6] or partially[7-9] heated from below, have also been reported. The resulting flow patterns were found to be considerably affected by the geometric shape of the system under consideration.

Interest in the study of natural convection heat transfer in repetitive geometries heated from below is relatively recent. Such studies furnish a useful description of the behaviour of fluids in several situations encountered. In fact, the increasing demand for the design of high packaging density has resulted in a change of the role of cooling in electronic industries. Since proper cooling of electronic components by natural or mixed convection is a reliable operation, the study of heat transfer resulting in these configurations must be examined in detail in order to provide adequate cooling and to prevent failure of the components. Among the older investigations concerning the repetitive geometries are the efforts of Jacobs *et al.*[10] who considered the case of a fluid mass of infinite extent above an array of uniformly spaced rectangular cavities. The bottom of the cavities was assumed to be isothermal with either adiabatic or isothermal side walls. The problem was studied experimentally and numerically for Grashof numbers ranging from 1 to 10^5, where the Grashof number is calculated based on the cavity width. The same problem was reconsidered by Jacobs and Mason[11] where the bottom of the cavities is subject to a uniform heat flux rather than constant temperature. It was found that the uniform heat flux condition leads to the development of strong secondary flow circulation cells and, ultimately, to a reversal flow in the cavity. It was pointed out that the heat transfer is greatly inhibited by the secondary cells for Grashof numbers greater than 10^3.

In their numerical approach and, owing to the symmetry of the problem, Jacobs *et al.*[10,11] restricted the calculations to the half of the smallest representative domain. This simplification forced the solution to be symmetric. Also the governing equations were solved in their steady-state form[11]. With these assumptions, the resulting flow pattern for a given set of governing parameters is unique. However, it was demonstrated recently that some natural convective flows may show multiple steady-state solutions[12-15]. Recently, Hasnaoui *et al.*[16] have extended the above studies concerning heat transfer, from an infinite uniform array of open cavities heated from below, to a situation where the flow is confined by a horizontal cold plate. They pointed out that the symmetry of the flow can be destroyed. The evolutionary path to steady-state flow was examined and sustained oscillatory behaviour was observed in several cases.

The objective of the present study is to gain some insight into fluid motion and heat transfer phenomena in the case of a finite number of cavities (two and three) covered by a cold plate and connected by adiabatic walls. The effects of the confining adiabatic walls and the connecting wall heights will be investigated. Comparison of the present results in terms of flow structure and average Nusselt number will be made with other published results.

Physical model and governing equations

The schematic representations of the geometric arrangements are depicted in Figure 1. They consist of a set of two and three cavities heated from below and connected by adiabatic walls. The hot and the cold walls are at isothermal temperatures T'_H and T'_C respectively. All the physical properties of the fluid are constant except the density in the buoyancy term where it obeys the Boussinesq approximation. It is assumed that the third dimension of the cavities is large enough so that the flow and heat transfer are two-dimensional. Using current hypothesis, the dimensionless governing equations in terms of vorticity Ω, temperature T and stream function Ψ are:

$$\frac{\partial \Omega}{\partial t} + \frac{\partial (u\Omega)}{\partial x} + \frac{\partial (v\Omega)}{\partial y} = Pr\left(\frac{\partial^2 \Omega}{\partial x^2} + \frac{\partial^2 \Omega}{\partial y^2}\right) - RaPr\left(\cos\Phi \frac{\partial T}{\partial x} - \sin\Phi \frac{\partial T}{\partial y}\right) \quad (1)$$

$$\frac{\partial T}{\partial t} + \frac{\partial (uT)}{\partial x} + \frac{\partial (vT)}{\partial y} = \left(\frac{\partial^2 T}{\partial x^2} + \frac{\partial^2 T}{\partial y^2}\right) \quad (2)$$

$$\frac{\partial^2 \Psi}{\partial x^2} + \frac{\partial^2 \Psi}{\partial y^2} = -\Omega \quad (3)$$

$$u = -\frac{\partial \Psi}{\partial y} \quad v = \frac{\partial \Psi}{\partial x} \quad (4)$$

The hydrodynamical boundary conditions are such that normal and tangential velocities vanish on all solid boundaries ($u = v = \Psi = 0$).

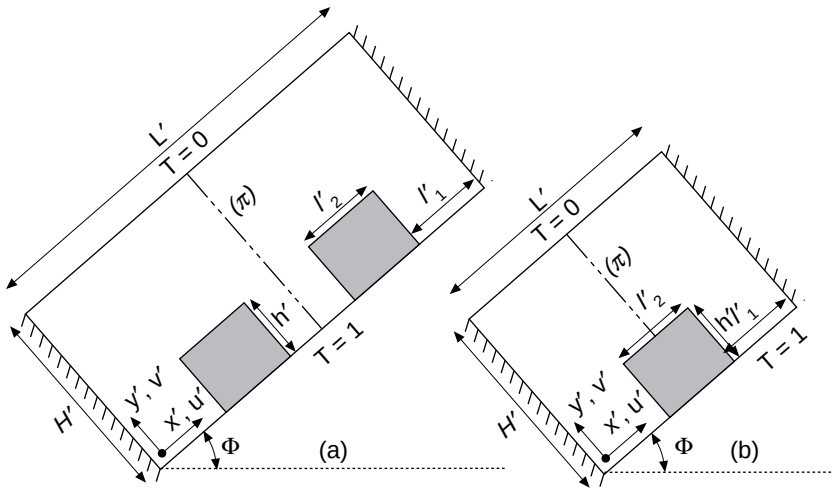

Figure 1.
Schematic of the physical problem: (a) case of three cavities; and (b) case of two cavities

The thermal boundary conditions for the case of three cavities are given by:

$$\left.\begin{aligned} &T = 0 \quad \text{for} \quad y = 1 \quad \text{and} \quad 0 \le x \le A = 5/2 \\ &T = 1 \quad \text{for} \quad y = 0 \quad \text{and} \quad 0 \le x \le 1/2 \\ &\qquad\qquad\qquad\qquad\quad 1 \le x \le 3/2 \\ &\qquad\qquad\qquad\qquad\quad 2 \le x \le 5/2 \end{aligned}\right\} \tag{5}$$

The thermal boundary conditions for the case of two cavities are given by:

$$\left.\begin{aligned} &T = 0 \quad \text{for} \quad y = 1 \quad \text{and} \quad 0 \le x \le A = 3/2 \\ &T = 1 \quad \text{for} \quad y = 0 \quad \text{and} \quad 0 \le x \le 1/2 \\ &\qquad\qquad\qquad\qquad\quad 1 \le x \le 3/2 \end{aligned}\right\} \tag{6}$$

$\frac{\partial T}{\partial n} = 0$ for insulated walls

where n denotes the normal direction to a given wall.

The normalized mean Nusselt number, which gives the net heat transfer rate leaving the system through the cold surface, is given by:

$$Nu = \frac{\bar{h}.H'}{\lambda} = \frac{Q}{Q_C} = \frac{1}{Q_C A}\int_0^A \left.\frac{\partial T}{\partial y}\right|_{y=1} dx \tag{7}$$

where Q_C denotes the overall heat transfer by conduction across the cooled wall.

Numerical method

The governing equations (1)-(3) describing the flow and heat transfer in this problem were solved numerically using a finite difference discretization procedure. Central difference formulae were used for all spatial derivative terms in the Poisson, energy, and vorticity equations. Discretized forms of temperature and vorticity equations were solved by using a modified alternate direction implicit method (ADI). This method has been extensively used in the past to solve transient two-dimensional problems. Values of the stream function at all grid points were obtained with equation (3) via a successive over relaxation method (SOR). Variations by less than 10^{-4} over all grid points for the stream function was adopted as the convergence criterion at each time step in order to satisfy the continuity equation. The time step size was varied from 2×10^{-5} to 10^{-4} depending on the Rayleigh number (Ra) and B. Uniform grids of 81×33 and 61×33 in x and y directions were found to model accurately the fluid flow and heat transfer respectively for the cases of three and two cavities. In fact, the effect of the grid size on heat transfer and fluid flow was examined by refining the mesh for both steady-state and most intense transient cases. The maximum differences

observed in the stationary regime were 2.3 per cent in Nu, and 0.86 per cent in Ψ_{ext} when grids of 121×65 were used. In transient cases, the maximum differences obtained by using the last grid were 2.8 per cent in $\overline{Nu}$, and 2 per cent in $\overline{\Psi}_{ext}$. The numerical model was validated with the solutions obtained by Hasnaoui *et al.*[16] and maximum deviations of 1 per cent were observed. The numerical code was also validated with the benchmark solution of De Vahl Davis and Jones[17]. For $Ra = 10^6$, the deviations were 0.5 per cent in Ψ_{max}, and 0.6 per cent in Nu_0.

Results and discussion

Flow fields, temperature fields, and heat transfer rates across a cold wall will be examined in the following sections for various Rayleigh numbers ($10^3 \leq Ra \leq 10^6$ and geometrical parameter B ($1/8 \leq B \leq 1/2$). The air was considered as a working fluid (Prandtl number, $Pr = 0.72$). All the analysis was carried out assuming $A = L'/H' = 2.5$ (for three cavities) and 1.5 (for two cavities) and an inclination angle Φ ranging from 0 to 180°.

Streamlines and isotherms ($\Phi = 0°$)

Case of three cavities. Typical results of streamlines and isotherms in the stationary regime are shown in Figure 2 for $B = 1/2$. For $Ra = 10^4$, Figure 2a

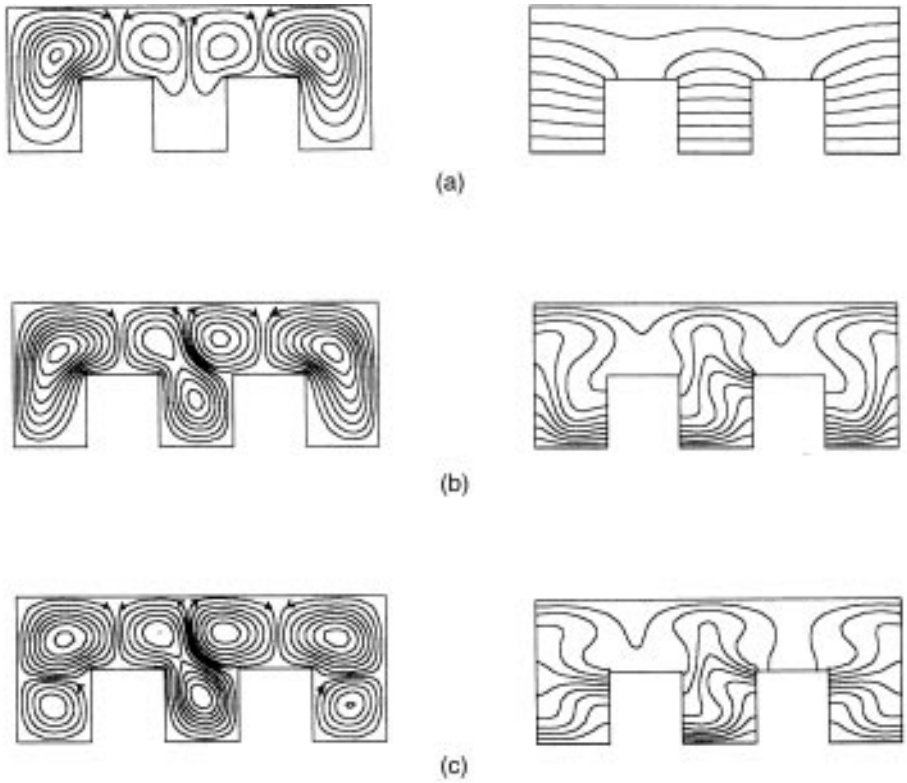

Figure 2.
Streamlines and isotherms for $B = 1/2$: (a) $Ra = 10^4$, $\Psi_{ext} = 1.41$; (b) $Ra = 5 \times 10^4$, $\Psi_{ext} = (7.43, -7.42)$; and (c) $Ra = 7 \times 10^4$, $\Psi_{ext} = (6.59, -7.00)$

shows that the flow regime is close to the pure conduction one. The fluid circulation is poor ($\Psi_{ext} = 1.41$). The isotherms are horizontal in the lower part of the central cavity and slightly distorted in the upper part. The flow pattern is characterized by a perfect symmetry about the vertical axis (π) which bisects the domain. The viscous forces exerted on the vertical adiabatic walls of the central cavity retard the motion in this cavity since the buoyancy forces are, for this Rayleigh number, insufficient to overcome the resistance forces. The aspects of the streamlines and isotherms aspects change significantly by increasing the Rayleigh number: the fluid circulation becomes more intense and the symmetry observed for smaller Rayleigh numbers is destroyed. Thus, for $Ra = 5 \times 10^4$, Figure 2b shows that the flow becomes asymmetric ($\Psi_{max} = 7.42$ and $\Psi_{min} = -7.43$) and the distortion of the isotherms expresses an increase in the heat transfer by natural convection. It is noted that the symmetry breaking occurs when Ra exceeds 1.75×10^4. A similar behaviour was observed by Hasnaoui *et al.*[16] in the case of an array of cavities. Also, as Figure 2c illustrates for $Ra = 7 \times 10^4$, each of the two big cells occupying the extreme cavities and the space above splits into two counter-rotating cells. The flow intensity and the heat leaving the domain across the cold horizontal boundary are directly affected by this break. This interesting phenomenon was not observed in the case of an array of cavities[16] since the effect of the confining walls was negligible. All the steady-state solutions were obtained for Rayleigh numbers $Ra \leq 5 \times 10^5$ while in the case of an array of cavities[16] the solutions remain steady for Ra up to 10^6. In the stationary regime, the results obtained for $B = 1/4$ (not presented here) were qualitatively similar to those observed for $B = 1/2$. However, the splitting of the cells in contact with the vertical confining walls was not obtained by increasing Ra.

It should be mentioned that whenever a steady-state asymmetric solution is possible, its mirror image is also a possible solution (Figure 3). This remark was also verified numerically by Hasnaoui *et al.*[16]. For $B = 1/4$, steady-state

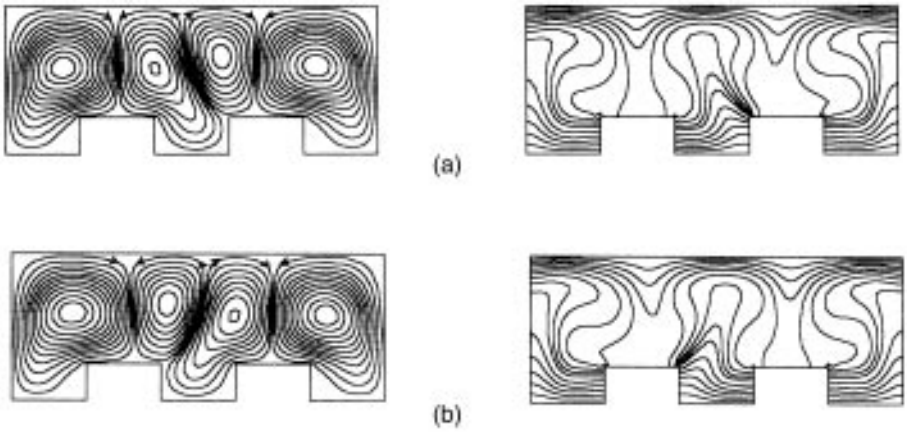

Figure 3.
Steady-state streamlines and isotherms for $B = 1/4$: two possible solutions for $Ra = 5 \times 10^4$: (a) $\Psi_{ext} = (10.25, -10.16)$; and (b) $\Psi_{ext} = (10.16, -10.25)$

solutions were observed for $Ra \leq 8 \times 10^4$. After this threshold value, sustained periodic solutions appeared. The transition points from steady-state to time-dependent flow were obtained by progressively increasing the Rayleigh number as follows: if a steady-state solution was obtained for Ra_1 and a transient one was obtained for $Ra_1 + \Delta Ra$, a third simulation is made by using $Ra_2 = Ra_1 + \Delta Ra/2$ and, depending on the new solution, the value of Ra_2 will be increased or decreased until a small difference exists between two successive Ra values for which steady-state and time-dependent modes are obtained. The solutions are characterized by periodic oscillations in time and their nature depends strongly on Ra. For $Ra = 8.5 \times 10^4$, Figure 4 shows the variations of Ψ_{max} (a) and Q (b) with time. These variations are sinusoidal with identical periods and give, by projection in the (Q, Ψ_{max}) phase plane, a P_1 solution (single closed curve) according to the convention of Lennie *et al.*[18] (Figure 4c). For $Ra = 10^5$, the

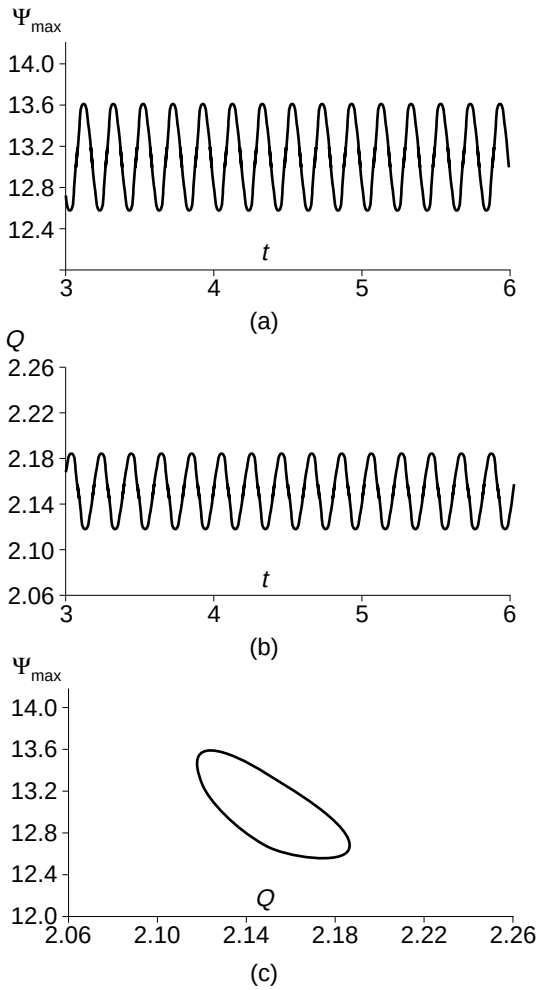

Figure 4.
Periodic solution for $Ra = 8.5 \times 10^4$ and $B = 1/4$: (a) Q variation with t; (b) maximum stream function variation with t; and (c) trajectory in the (Q, Ψ_{max}) phase plane

amplitudes of the oscillations increase (Figure 5a, b) and the shape of the variations changes significantly. The oscillations are more complicated with several peaks appearing in Ψ_{max}. The resulting trajectory in (Q, Ψ_{max}) phase plane is also a complicated closed curve as a result of the periodic variations of Ψ_{max} and Q with time (Figure 5c).

Figure 6 shows the streamlines and isotherm pattern at the times indicated by 1, 2, 3, …, 8 in Figure 5a during one flow cycle. It can be clearly seen that the fluid oscillates between two extreme positions. Each of the two principal cells located at the central cavity level (between the extreme cells) reaches its maximum size, consequently constraining the other central cell to be of

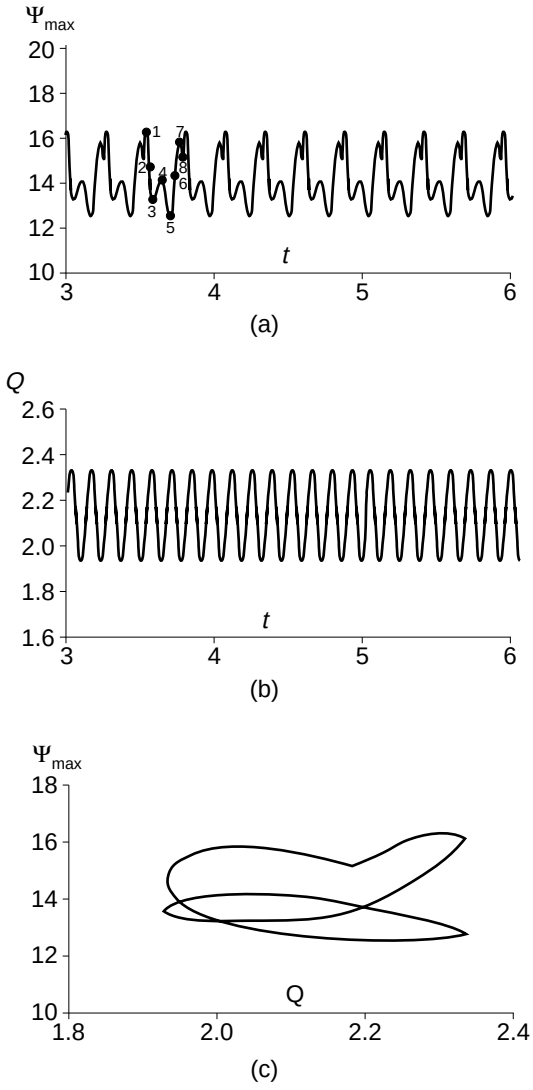

Figure 5. Periodic solution for $Ra = 10^5$ and $B = 1/4$: (a) Q variation with t; (b) maximum stream function variation with t; and (c) trajectory in the (Q, Ψ_{max}) phase plane

minimum size. This behaviour leads in each half of the flow cycle to the formation of a small eddy with the same sign as the poor cell. In the other half of the flow cycle, the eddy and the poor cell increase with time in detriment of the "main cell" and subsequently merge, forcing it to liberate the lower part of the central cavity.

The decrease in the height of the vertical adiabatic blocs corresponds to reducing the geometrical parameter B. Thus, for $B = 1/8$ all the solutions obtained in a stationary regime remain symmetrical with respect to the vertical axis (π) while the symmetry is destroyed for $B = 1/2$ and 1/4 by increasing Ra. Typical streamlines and isotherms illustrating these observations are presented in Figures 7a and 7b for $Ra = 10^4$ and 10^5 respectively. A comparison with the corresponding cases with higher values of B reveals more intense circulations ($\Psi_{ext} = 4.92$ and 17.81). The value of Ra for which the steady-state solution was reached is $Ra \simeq 1.75 \times 10^5$. Above this limit, the solutions are transient with

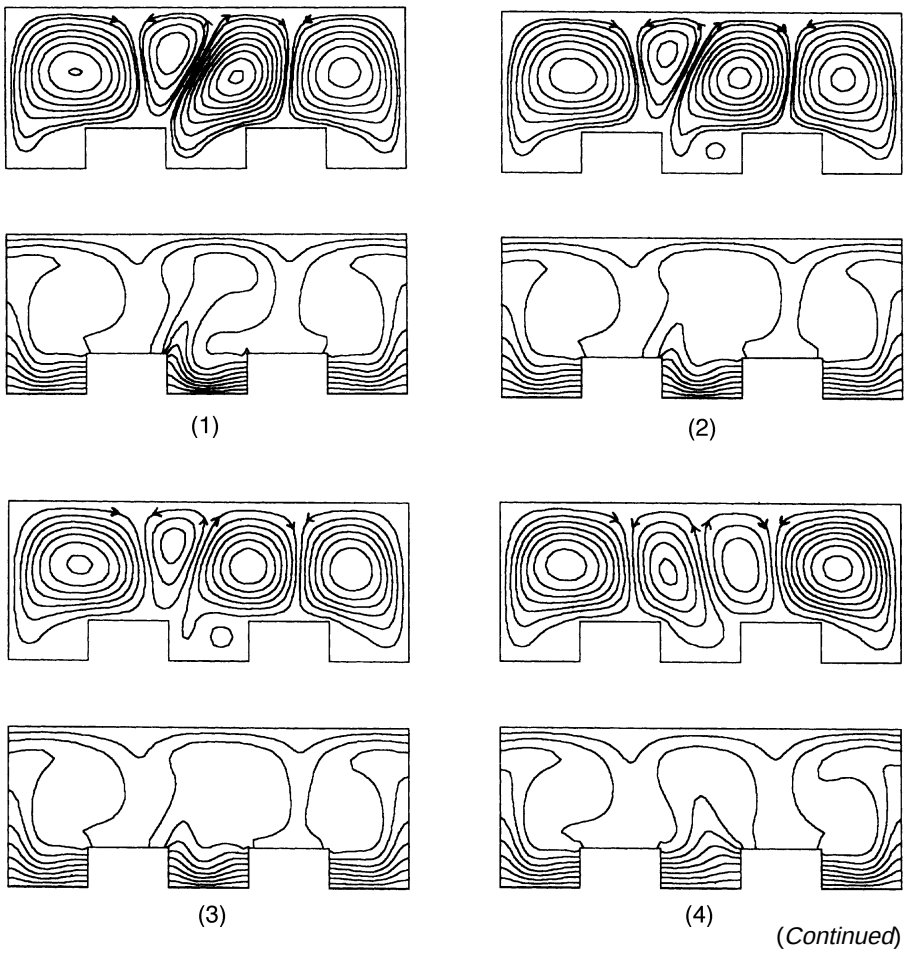

Figure 6.
Streamlines and isotherms over one cycle for $Ra = 10^5$ and $B = 1/4$: (1) $\Psi_{ext} = (16.35, -12.94)$; (2) $\Psi_{ext} = (14.74, -12.57)$; (3) $\Psi_{ext} = (13.45, -12.88)$; (4) $\Psi_{ext} = (14.25, -15.91)$; (5) $\Psi_{ext} = (12.52, -14.70)$; (6) $\Psi_{ext} = (14.70, -13.84)$; (7) $\Psi_{ext} = (15.97, -14.24)$; and (8) $\Psi_{ext} = (14.98, -13.60)$

(*Continued*)

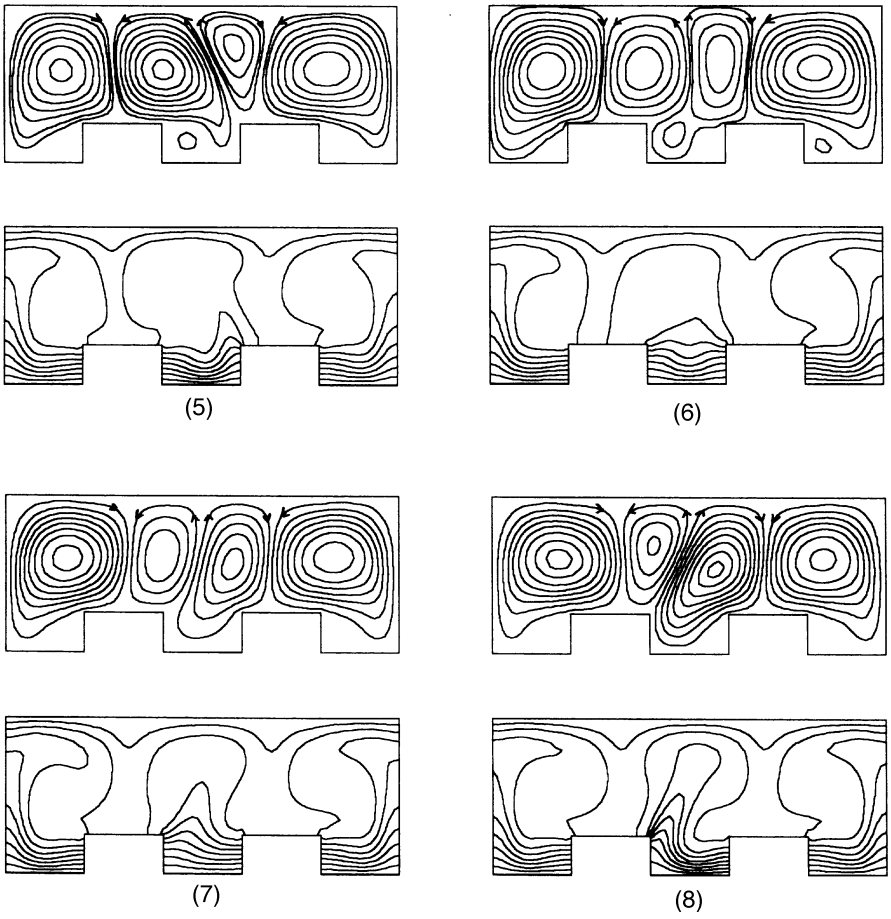

Figure 6.

sinusoidal variations for Ψ_{max} and Q as shown in Figures 8a and 8b for $Ra = 2 \times 10^5$. Since the periods of the oscillations are identical, the corresponding trajectory in the phase space is a single closed curve as shown in Figure 8c. Chaotic behaviour is also presented in Figures 9a and 9b for $Ra = 5 \times 10^5$. The fluctuations are larger in magnitude, indicating a better circulation. In order to identify the route of transition to chaotic motion, a spectral analysis was used. It was found that at the beginning of the periodic motion ($Ra = 2.25 \times 10^5$), only one fundamental frequency is present ($f_0 = 4.8828$). On progressively increasing Ra, subharmonic frequencies ($f_0/2$ and $f_0/4$) appeared and the transition to chaotic regime occurred via a subharmonic bifurcations as reported by Gollub and Benson[19]. It is also interesting to mention that the transition to chaotic convection occurred in a similar fashion for $B = 1/4$ with almost the same fundamental frequency. A summary of the principal transitions obtained in the case of three cavities and different values of B is presented in Table I.

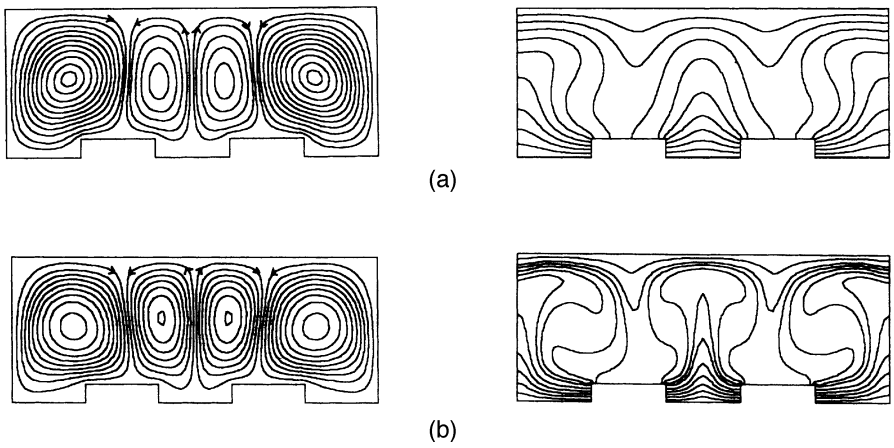

Figure 7.
Typical streamlines and isotherms for $B = 1/8$: (a) $Ra = 10^4$; $\Psi_{ext} = 4.92$; and (b) $Ra = 10^5$; $\Psi_{ext} = 17.81$

Case of two cavities. The results obtained in the case of two cavities differ significantly from those of three and an array of cavities. The first point to note here is that the symmetry of the steady-state solutions with respect to the vertical axis (π) persists independently of the cavity height B.

The case of $B = 1/2$ is characterized by a bicellular pattern consisting of two counter-rotating cells for $Ra \leq 6 \times 10^4$. After this threshold value of Ra, a quadracellular mode was observed and persisted for Rayleigh numbers lower than 4.75×10^5. The multiplicity of the solutions was briefly examined. For $Ra = 6 \times 10^4$, two final steady-state solutions were obtained by using appropriate initial conditions. The first solution is bicellular (Figure 10a) but cannot survive for higher Ra. The second solution, which is stable for higher Ra, is quadracellular (Figure 10b). The corresponding normalized Nusselt numbers are respectively 2.51 and 1.92. This is expected since a break of the cells affects the general circulation of the fluid. For $Ra > 4.75 \times 10^5$, sustained sinusoidal solutions of P_1 type were obtained. Different behaviours have been observed for $B = 1/2$ and higher numbers of cavities.

For all the steady state solutions obtained for $B = 1/4$ and $Ra \leq 10^5$, the flow pattern remains principally bicellular and symmetrical with a weak vortex in the vicinity of the adiabatic vertical walls of the cavities as shown in Figure 11 for $Ra = 10^5$. For $Ra > 10^5$ periodic solutions were obtained. Thus for $Ra = 6 \times 10^5$, the flow motion is characterized by periodic variations of Ψ_{max} and Q with time. The relative corresponding behaviours (Figures 12a and 12b) show that each of these curves presents principal and secondary peaks per period ($\Psi_{max} = 53.2$ and $Q_{max} = 5.25$). The corresponding trajectory in the phase space is a closed curve as shown in Figure 12c. For $Ra \geq 7 \times 10^5$, a non periodic convection was observed.

For smaller values of B, i.e. $B = 1/8$, the steady-state symmetrical solutions were obtained for $Ra \leq 3.75 \times 10^5$. Above this limit the fluid flow was dominated by non-periodic convection. A spectral analysis of the results (not presented

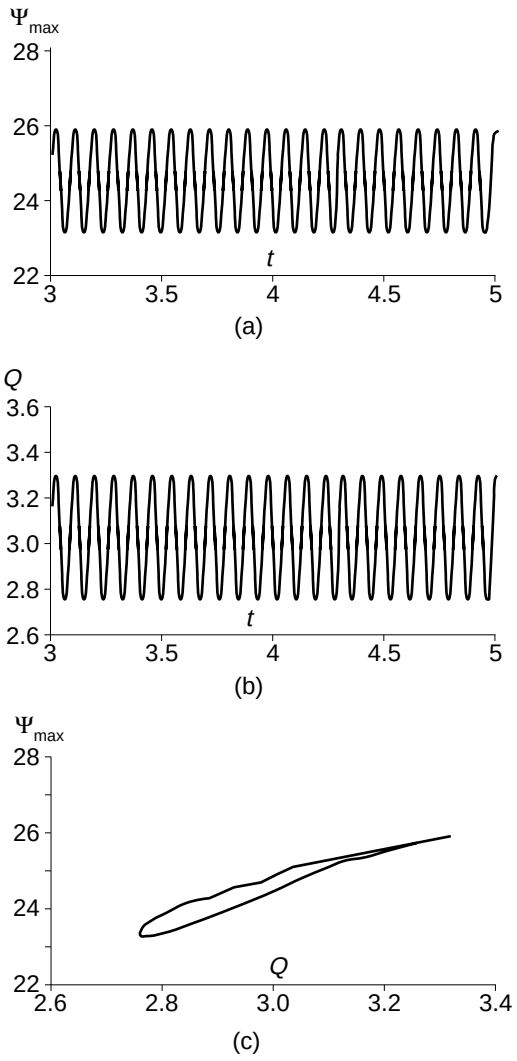

Figure 8.
Periodic solution for $Ra = 2 \times 10^5$ and $B = 1/8$: (a) Q variation with t; (b) maximum stream function variation with t; and (c) trajectory in the (Q, Ψ_{max}) phase plane

here) showed that the flow regime is neither periodic nor chaotic. This behaviour was not encountered in the case of a large number of cavities. This may be a consequence of the decrease of the relative height of the cavities conjugated with the confining vertical plates.

Heat transfer

The main quantity of practical interest is the normalized mean Nusselt number *Nu*. It gives the ratio of the amount heat transferred across the cold wall of the cavity to the one transferred by pure conduction. The *Nu* variations with *Ra* are presented in Figure 13 for various numbers of the cavities. For $B = 1/8$, Figure 13a shows that the Rayleigh numbers for which the convection mode arises, in

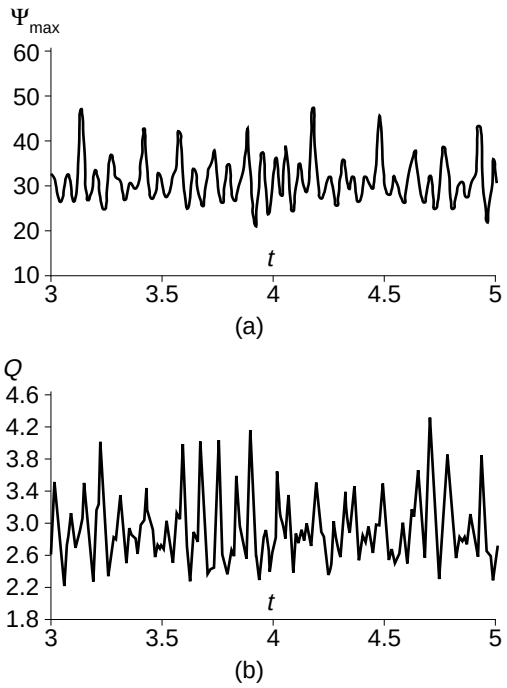

Figure 9.
Chaotic flow regime for $Ra = 5 \times 10^5$ and $B = 1/8$: (a) Q variation with t; and (b) maximum stream function variation with t

contrast to heat transfer, increase with the number of cavities. Also, the steady-state regime is maintained in the case of two cavities until $Ra \simeq 3.75 \times 10^5$. By increasing the parameter B to 1/4, similar behaviours can be observed as shown in Figure 13b. However, the stationary regime in the case of two cavities

B	Ra	Nature of the solutions
	$Ra \leq 1.75 \times 10^4$	Symmetrical
1/2	$1.75 \times 10^4 < Ra \leq 5.10^5$	Dissymmetrical
	$Ra > 5.10^5$	Non-periodic solutions
	$Ra \leq 9.10^3$	Symmetrical
	$9.10^3 < Ra \leq 8.10^4$	Dissymmetrical
1/4	$8.5 \times 10^4 \leq Ra \leq 9.75 \times 10^4$	Sinusoidal (P_1)
	$10^5 \leq Ra \leq 2.10^5$	Periodic
	$Ra \geq 5.10^5$	Chaotic
	$Ra \leq 1.75 \times 10^5$	Symmetrical
1/8	$2.10^5 \leq Ra \leq 3.5 \times 10^5$	Sinusoidal (P_1)
	$3.75 \times 10^5 \leq Ra \leq 4.75 \times 10^5$	Transition to a chaotic regime
	$Ra \geq 5.10^5$	Chaotic

Table I.
Flow characteristics in the case of three cavities

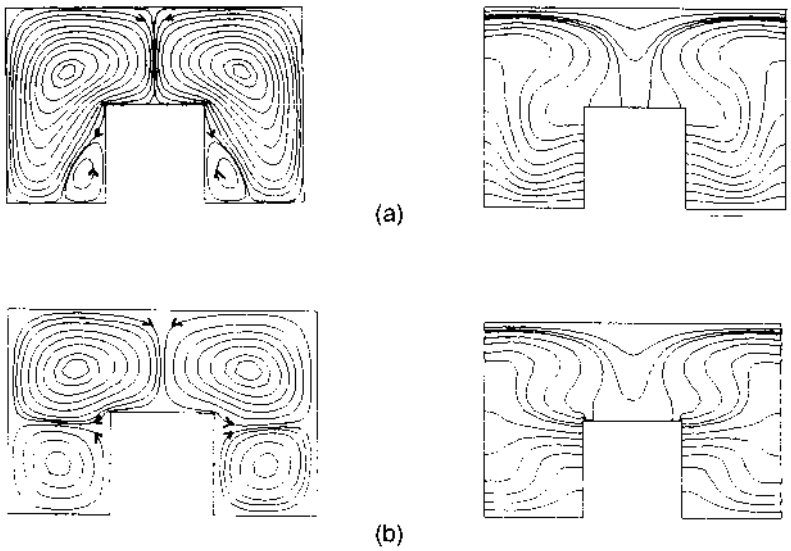

Figure 10. Two possible solutions for $Ra = 6 \times 10^4$ and $B = 1/2$: (a) $\Psi_{ext} = 7.57$; and (b) $\Psi_{ext} = 5.81$

disappears earlier (for $Ra > 10^5$). Further increase in B induces similar trends only for $Ra \leq 4.5 \times 10^4$ as shown in Figure 13c for $B = 1/2$. The principal difference noted in this range of Ra is the delay in the appearance of the convection. For $Ra \leq 6 \times 10^4$, the splitting phenomenon of the cells occurring in the cases of two and three cavities considerably affects the behaviour of the Nusselt number. It induces a further increase in the viscous forces between the vortices located at the extreme cavities. Consequently, the corresponding Nusselt numbers decrease in small ranges of Ra. As Ra exceeds 8×10^4 the Nusselt numbers for three and an infinite number of cavities are identical and higher than those obtained in the case of two cavities. This tendency is also maintained in transient periodic convection. The mean values of the Nusselt number, obtained by integration over one flow cycle, are shown in these figures as filled circles.

In order to investigate the effect of the inclination of the cavities on heat transfer, various simulations were conducted for $Ra = 10^5$ and Φ ranging from 0 to 180°. Figure 14a shows the variations of Nu with Φ for different values of B in the case of three cavities. It can be seen from this figure that Nu depends strongly on B and Φ. For $10° < \Phi < 100°$, the heat transfer is an increasing function of B.

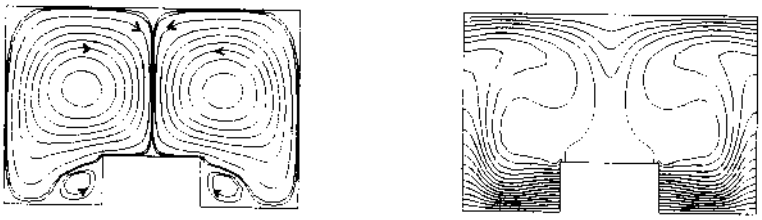

Figure 11. Streamlines and isotherms for $Ra = 10^5$ and $B = 1/4$: $\Psi_{ext} = 14.02$

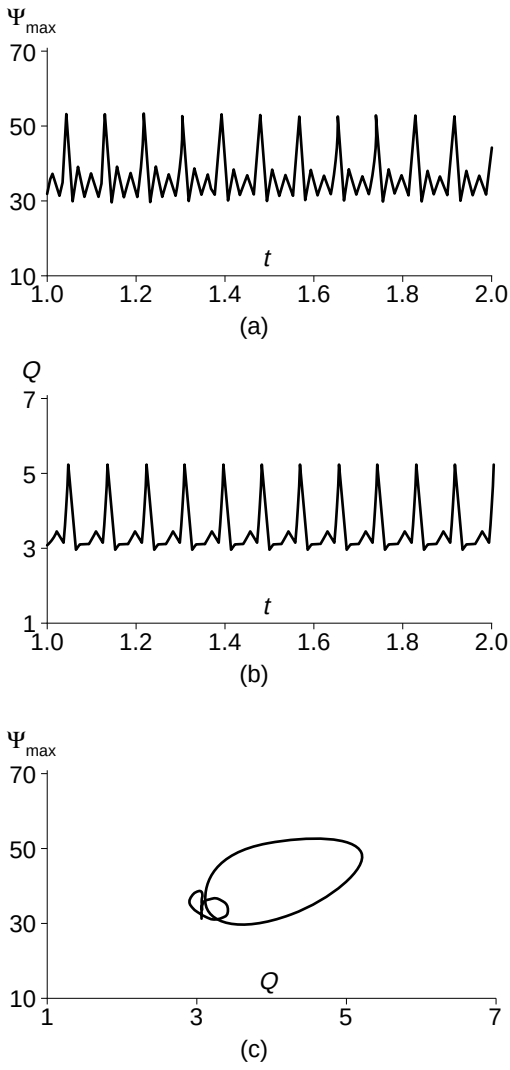

Figure 12.
Periodic solution for $Ra = 6 \times 10^5$ and $B = 1/4$: (a) maximum stream function variation with t; (b) Q variation with t; and (c) trajectory in the (Q, Ψ_{max}) phase plane

Outside this range of Φ, the Nusselt number increases with decreasing B. The absolute maximum of Nu is obtained for $B = 1/2$ and $\Phi = 50°$. The case of $\Phi = 180°$ (system heated from above) is characterized by the pure conduction regime. For $B = 1/4$, the fluid flow is periodic for $\Phi = 0°$. The reported value in this case corresponds to a mean value of Nu obtained by integration of the instantaneous Nu over one period of the flow. Similar behaviours are obtained in the case of two cavities as it can be seen from Figure 14b. The lower limit of Φ for which the heat transfer increases with B is 20°. The absolute maximum of Nu is also obtained for $B = 1/2$ but for $\Phi = 70°$ in this case.

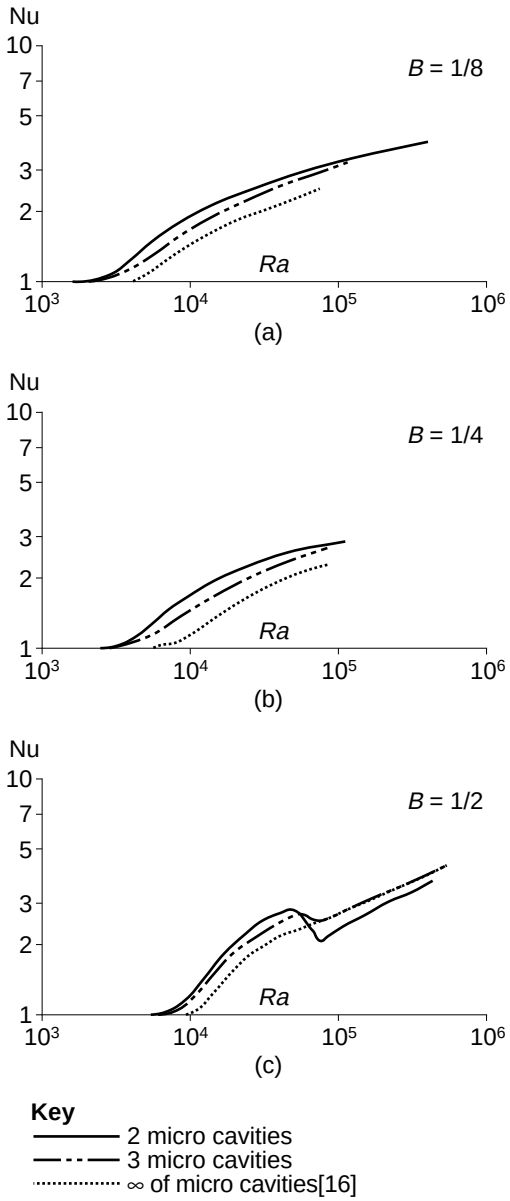

Figure 13. Variation of the normalized mean Nusselt number *Nu* with *Ra* for various numbers of the cavities: (a) $B = 1/8$; (b) $B = 1/4$; and (c) $B = 1/2$

Conclusion

A numerical study of the natural convection heat transfer in the case of two and three cavities heated from below was conducted. Steady-state periodic and chaotic solutions were obtained for different combinations of the governing parameters. The influence of the relative height of the cavities on the fluid flow and heat transfer was then illustrated. It was found that the symmetry of the

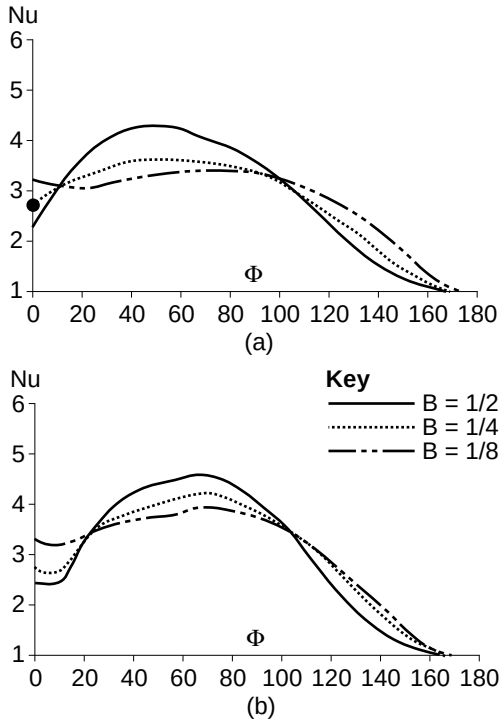

Figure 14.
Variation of the normalized mean Nusselt number Nu with Φ for $Ra = 10^5$ and various B: (a) case of three cavities; and (b) case of two cavities

solutions is considerably affected by the relative height of the cavities and their number. This symmetry is destroyed for $B > 1/8$ in the case of a system formed by more than two cavities. Periodic solutions and chaotic behaviours have also been obtained for $B \leq 1/4$. These trends have not been obtained in the case of

B	Ra	Nature of the solutions
1/2	$Ra \leq 4.75 \times 10^5$	Symmetrical
	$5 \times 10^5 \leq Ra \leq 7.7 \times 10^5$	Sinusoidal (P_1)
	$Ra > 8.10^5$	Non-periodic solutions
1/4	$Ra \leq 10^5$	Symmetrical
	$1.25 \times 10^5 \leq Ra \leq 1.35 \times 10^5$	Sinusoidal (P_1)
	$1.4 \times 10^5 \leq Ra \leq 3.5 \times 10^5$	Periodic (P_2)
	$4.10^5 \leq Ra \leq 5.5 \times 10^5$	Non-periodic solutions
	$6.10^5 \leq Ra \leq 6.75 \times 10^5$	Periodic (> P_2)
	$Ra \geq 7.10^5$	Non-periodic solutions
1/8	$Ra \leq 3.75 \times 10^5$	Symmetrical
	$Ra \geq 4.10^5$	Non-periodic solutions

Table II.
Flow characteristics in the case of two cavities

two cavities since a perfect symmetry of the solutions about the vertical axis π was found for all the *Ra* values considered. Also, it was found that the normalized mean Nusselt number is a decreasing function of the number of cavities in the absence of the break of the extreme cells.

References

1. Bejan, A., *Convection Heat Transfer,* John Wiley, New York, NY, 1984.
2. Platten, J.K. and Legros, J.C., *Convection in Liquids,* Springer-Verlag, New York, NY, 1984.
3. Yang, K.T., "Natural convection in enclosures", in Kakac, S., Shah, R. and Aung, W. (Eds), *Hand Book of Single Phase Convective Heat Transfer*, New York, NY, 1987.
4. Catton, I., "Natural convection in enclosures", *Proceedings of the 6th International Heat Transfer Conference,* Vol. 6, Toronto, 1979, pp. 13-43.
5. Catton, I., "Effect of wall conduction on the stability of a fluid in a rectangular region heated from below", *J. Heat Transfer*, Vol. 94, 1972, pp. 446-52.
6. Oertel, H., "Steady and time dependent convection in a rectangular box", *Sixth International Heat Transfer Conference*, Vol. 2, 1978, pp. 281-6.
7. Torrance, K.E., "Natural convection in thermally stratified enclosures with localized heating from below", *J. Fluid Mech.*, Vol. 95, 1979, pp. 477-95.
8. Kamotani, Y., Wang, L.W. and Ostrach, S., "Natural convection heat transfer in a water layer with localized heating from below", *21st National Heat Transfer Conference.,* Seattle, HTD, Vol. 26, 1983, pp. 43-8.
9. Fusegi, T. and Farouk, B., "Natural convection in a thermally stratified square cavity with localized heating from below", *23rd AIChE National Heat Transfer Conference*, Denver, CO, Paper 85-HT-34, 1985.
10. Jacobs, H.R., Mason, W.E. and Hikida, E.T., "Natural convection in open rectangular cavities", Paper NC 3.2, *Heat Transfer,* Vol. 3, 1974, pp. 90-4.
11. Jacobs, H.R. and Mason, W.E., "Natural convection in open cavities with adiabatic side-walls", *Proceedings Heat Transfer and Fluid Mechanical Institute,* Stanford University Press, 1976, pp. 33-46.
12. Robillard, L., Wang, C.H. and Vasseur, P., "Multiple steady states in a confined porous medium with localized heating from below", *Num. Heat Transfer*, Vol. 13, 1988, pp. 91-110.
13. Caltagirone, J.P. and Bories, B., "Solutions and stability criteria of natural convective flow in an inclined porous layer", *J. Fluid Mech.,* Vol. 155, 1985, pp. 267-87.
14. Moya, S.L., Ramos, E. and Sen, M., "Numerical study of natural convection in a tilted rectangular porous material", *Int. J. Heat Mass Transfer*, Vol. 30, 1987, pp. 741-56.
15. Sen, M., Vasseur, P. and Robillard, L., "Multiple steady states for unicellular natural convection in an inclined porous layer", *Int. J. Heat Mass Transfer*, Vol. 30, 1987, pp. 2097-113.
16. Hasnaoui, M., Bilgen, E. and Vasseur, P., "Natural convection above an array of open cavities heated from below", *Num. Heat Transfer,* Part A, Vol. 18, 1990, pp. 463-82.
17. De Vahl Davis, G. and Jones, I.P., "Natural convection in a square cavity: a comparison exercise", *Int. J. Num. Meth. Fluids*, Vol. 3, 1983, pp. 227-48.
18. Lennie, T.B., McKenzie, D.P., Moore, D.R. and Weiss, N.O., "The break-down of steady convection", *J. Fluid Mech.,* Vol. 188, 1988, pp. 47-85.
19. Gollub, J.P. and Benson, S.V., "Many routes to turbulent convection", *J. Fluid Mech.*, Vol. 100, Part 3, 1980, pp. 449-70.